THE EFFECT OF FREQUENCY ON CYCLIC CRACK GROWTH IN 200 MARAGING STEEL IN A SALT WATER ENVIRONMENT

R. Eisenstadt* and D. L. Smail**

INTRODUCTION

The rotating beam understressing technique [1] for generating crack propagation data was used to show that a specimen of 200 maraging steel in a salt water environment shows a factor of 10 increase in crack growth rate at a frequency of 3.3 Hz (200 rpm) compared to 0.017 Hz (1 rpm). The rotating beam understressing technique has been shown to be quire reliable and inexpensive. As the crack grows in the beam, the uncracked area decreases and for a given moment, the stress intensity factor increases. The stress intensity factor will increase to a maximum value at which time the material will fracture. This maximum stress intensity factor is a property of the material. Crack growth rate is also a function of the stress intensity value [3].

EQUIPMENT AND PROCEDURE

The large rotating bending machine, located at Union College and used in these experiments, is a converted lathe. The specimens are 25.4 mm in diameter and approximately 0.127 m long. The specimen has a circumferential groove machined around the centre. The groove is 60-deg., 1.27 mm deep with a root radius of less than 0.025 mm.

The load beam is a 1.27 m long hollow pipe with an enlarged end which has 0.05 m opening. The specimen and collet is held in this opening of the load beam by tightening the lock nut at the end of a 15.9 mm diameter draw rod, which is threaded into one end of the specimen. A large bearing is attached at the load end of the specimen and another at the end of the load beam opposite the specimen. From this bearing the load is hung. A short draw rod is threaded into the opposite end of the specimen and is used to tighten the specimen and collet into the drive unit. A microswitch mounted on the drive unit provides a record of the number of stress cycles. Variable speeds are obtained by changing the size and number of pulleys in the drive train.

To provide a corrosive environment, the specimens were mounted in a salt water box. The specimen is inserted through holes in the side of the box and sealed with O-rings and rubber bands. A 4% salt water solution was pumped in through a hole in the top of the salt water box and drained out through a hole in the bottom. The specimen is kept immersed during the entire test by balancing the flows into and out of the box.

* Union College, Schenectady, New York, U. S. A.
** Knolls Atomic Power Laboratory, General Electric, Schenectady, New York, U. S. A.

The material tested during these experiments was 200 maraging steel. The steel is termed maraging steel because of the precipitation reaction which occurs during aging. This precipitation reaction accounts for its ultra-high strength. The four major requirements for a "perfect alloy" are strength, ductility, fabricability and corrosion resistance. Of these, 200 maraging steel lacks only corrosion resistance, especially when used in sea-water environments [4]. The material has the following composition: 18% Ni, 3.2% Mo, 0.2% Ti, 0.1% Al, 0.03% max. C, 8.5% Co, and the balance Fe.

200 maraging steel has an ultimate tensilt strength of 1372 MPa, a 13% elongation, a 60% reduction in area and a 0.2% yield strength of 1289 MPa. The test material was aged for 3 hours at 755 K.

The method used to obtain crack propagation data is known as the interrupted stressing technique [1]. After a known number of stress cycles, the bending moment on the specimen is decreased. If this decreased bending moment is low enough and the specimen is rotated long enough, a fine dark ring will be left on the broken specimen that will locate the tip of the crack. The crack propagation is then continued with the original bending moment. The lower moment (minor load), approximately 0.5 to 0.6 of the major load is selected so that the crack propagation rate is negligible but results in a clear mark.

A rough estimate of the number of stress cycles to failure at a given bending moment is estimated from the information obtained from running several trial specimens. If for a given speed and bending moment the number of stress cycles to failure was estimated to be 20,000 cycles, the fatigue test was interrupted at 10,000, 14,000, 16,000, 18,000, 19,000, and 20,000 cycles. At each of these interruptions, the major load was removed and the minor load was put on and run for 1,000 to 6,000 cycles. After the minor load had been run, the major load would be put back on the load beam and the specimen was run until the next scheduled interruption in the stress test. This was repeated until the specimen failed.

Figure 1 shows a specimen after it had failed. Note that the ring indicating the crack location can be seen clearly. Although the rings are eccentric, crack propagation data can be obtained successfully from the specimen by the use of the techniques described in the next section.

DATA ANALYSIS

The method used in comparing crack propagation data is to plot the crack growth rate versus the stress intensity factor. The following discussion gives the method used to obtain these values.

After the specimen is broken, the rings on the specimen locate the crack depth after a known number of stress cycles. The crack depth can be measured by several means. For these experiments, a Baush and Laumb microscope with a hundred division reticle was used. A line is scribed on the specimen to pass through the centre of the specimen and the centre of the fracture. Along this line the distances from the edge of the specimen to a particular ring on either side of the fracture are measured as shown in Figure 2 and are referred to as a_1 and a_2. The average crack depth $\bar{a} = (a_1+a_2)/2$; $a_1+a_2+2r = D$ where r is the radius of the uncracked material and D is the outside diameter of the specimen. The radius r can be determined from the following equation:

$$r = \frac{D}{2} - \bar{a} .$$

The eccentricity of the remaining uncracked material e is calculated from the following equation:

$$e = \frac{a_1 - a_2}{2} .$$

By measuring the slope of the plot of the average crack depth versus number of stress cycles, Figure 3, the crack growth rate, d(2a)/dN, can be determined.

Using a formula derived by Harris [5] for the maximum stress intensity factor adapted for solid round bars subjected to bending moments only, Eisenstadt [1] developed a formula for calculating the stress intensity factor with an eccentric crack front [6]. Eisenstadt's formula is

$$K_1 = \frac{2.257\ M}{r^3+4rd^2}\left(\frac{.80}{\bar{a}} + \frac{7.12}{r}\right)^{-1/2}$$

where M is the bending moment and $\bar{a}$ is the average crack depth from the surface. Since we would like to compare the data with those of Crooker and Lange for a zero to maximum stress condition, we must take into account that there is some crack growth due to compression. Eisenstadt [6] found that to obtain the effective stress intensity factor (K_{eff}) it was necessary to multiply K_{max} by $\sqrt{2}$ for a rotating beam.

DISCUSSION OF RESULTS

A curve of average radial crack length versus the number of stress cycles was drawn, see Figure 3. The slope of the tangent to the curve at each of the data points was determined. The slope of this tangent line gives us the average radial crack growth per stress cycle.

In Figure 4, the crack propagation rate versus the stress intensity factor is plotted. In this figure it can be seen that there is a very large effect of frequency on the crack propagation rate. At 3.3 Hz (200 rpm) the specimen broke in a short time. There was very little difference between running the specimen in a 4% salt water solution or running it in air. The difference between running the specimen at 0.17 Hz (1 rpm) in salt water resulted in a factor of ten increase in the crack propagation rate.

At speeds of 3.3 Hz (200 rpm) or greater, it was found that the salt water solution had little effect on the crack growth rate. It can be seen in Figure 5, that the curves for specimens numbered 18 and 21 are approximately the same as specimen number 20, even though numbers 18 and 21 were run in a 4% salt water solution and number 20 was run in the air.

Crooker and Lange [7] have worked extensively on fatigue-crack growth in high-strength steels. Figure 6 compares the results of Crooker and Lange with those obtained using the rotating beam understressing method. The relative effects at the lower frequencies are similar, but the magnitudes of the crack growth rates for the same stress intensity factor vary somewhat; about 2 times as high as the Union College data. In order to determine

whether the crack growth rates were of the correct order, a scatter band of results obtained by Barsom et al [8] for crack growth in air in Hy 80, 130, 10 and 12 Cr steels was superimposed on the results as shown on Figure 4. It appears that the results in air and in room temperature salt water at 3.3 Hz fall within the band. Further agreement was obtained from reference [6] for 12 Cr steel at 10 Hz in both air and 20°C salt water as shown on Figure 5.

CONCLUSIONS

1) The difference in crack growth rate at stress intensity values of 22 to 110 MPa.$m^{1/2}$ is about 10 to 1 for speeds of 0.017 Hz (1 rpm) to 3.3 Hz (200 rpm) in 200 maraging steel in a 4% salt water solution at room temperature for the same stress intensity range.

2) The crack growth rate more than doubles as frequency is reduced from 3.3 Hz (200 rpm) to 0.044 Hz (2.64 rpm).

3) The crack growth rate more than triples as frequency is reduced from 0.044 Hz (2.64 rpm) to 0.017 Hz (1.0 rpm).

REFERENCES

1. EISENSTADT, R. and FULLER, W., J. of Basic Eng., Trans. ASME, Series D, 92, 1970, 1.
2. CLARK, W. G., Jr. and HUDAK, S. J., Jr., ASTM E-24.04.01 Task Group Report, 1973.
3. PARIS, P. C., Proceedings of the 10th Sagamore Army Materials Research Conference, Syracuse University Press, 1964.
4. CONTRACTOR, G. P., J. of Metals, August, 1966.
5. HARRIS, D. O., J. of Basic Eng., ASME, 1967.
6. EISENSTADT, R. and RAJAN, K. M., J. of Materials, ASME, 1974.
7. CROOKER, T. W. and LANGE, E. A., ASTM STP 462, 1970, 258-271.
8. BARSOM, J. M., IMHOF, E. J. and ROLPHE, S. T., Eng. Frac. Mech., 2, 1971, 301-317.

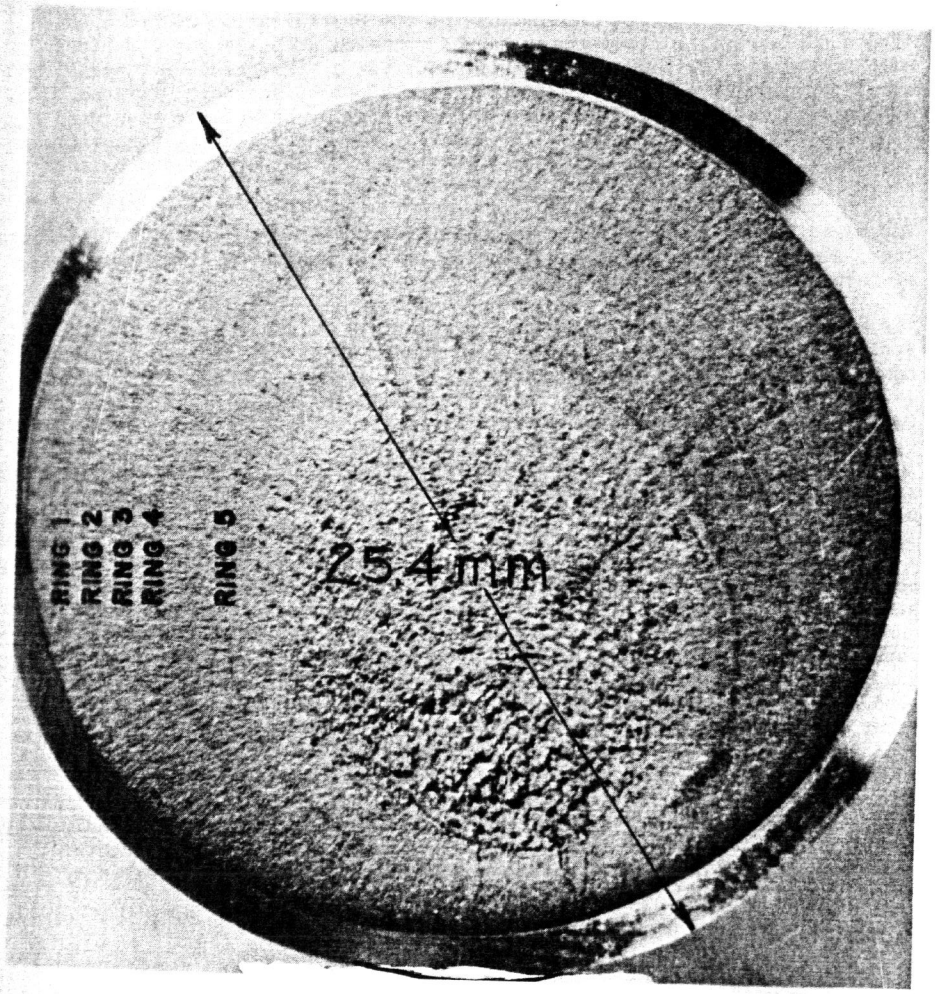

Figure 1 Fracture Specimen Exhibiting Rings at Points of Load Reduction

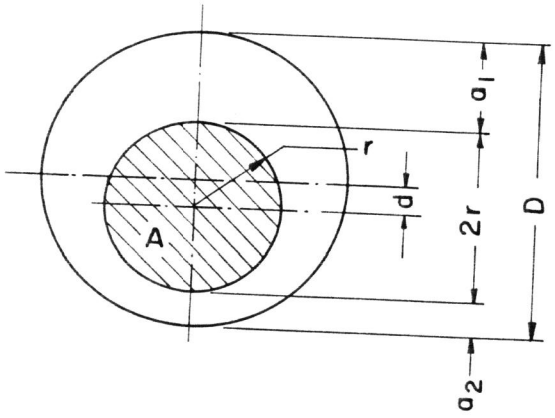

Figure 2 Schematic Fracture Surface

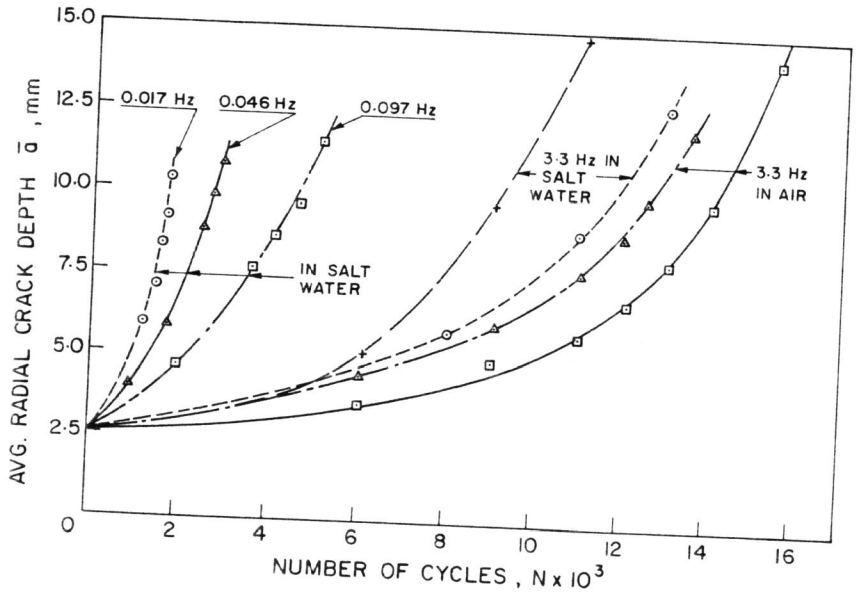

Figure 3 Crack Depth versus Number of Cycles, the Effects of Frequency and Environment

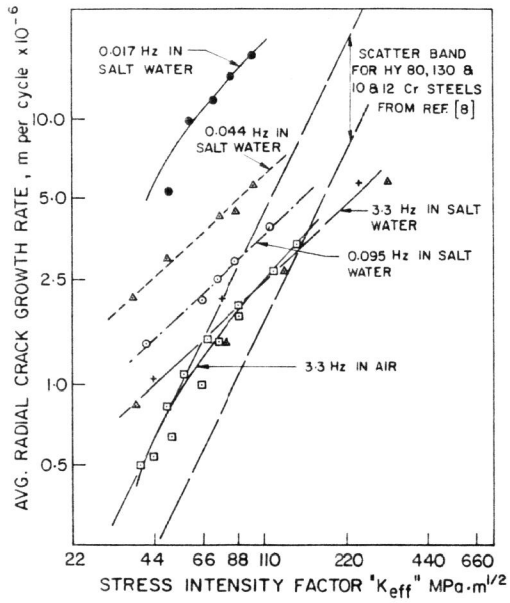

Figure 4 Crack Growth Rate versus Effective Stress Intensity Factor, the Effects of Frequency and Environment

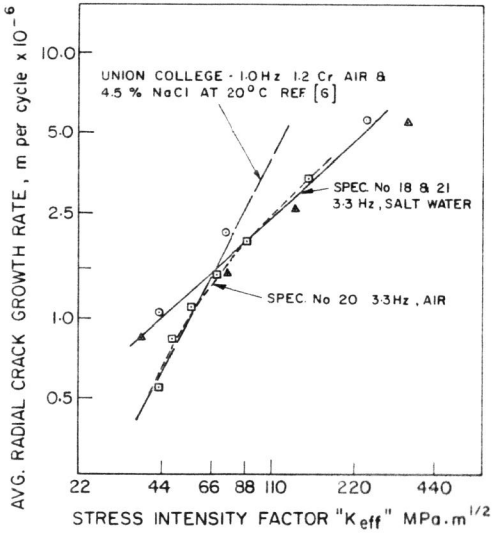

Figure 5 Crack Growth Rate versus Effective Stress Intensity Factor, the Effect of Environment at 3.3 Hz

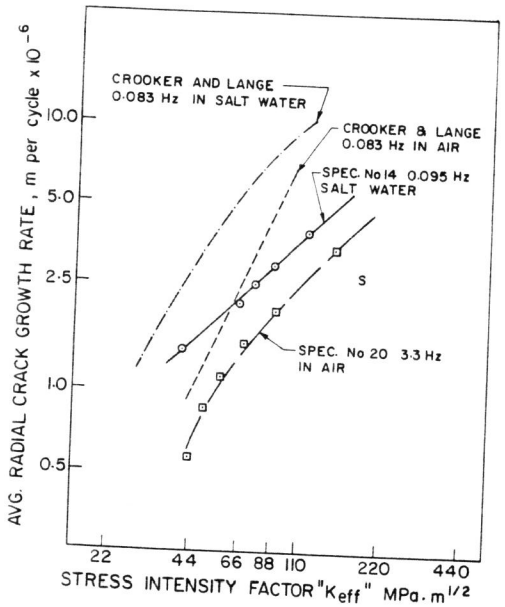

Figure 6 Crack Growth Rate versus Effective Stress Intensity Factor, Comparison of Current Data with that of Crooker and Lange [7]